Machine learning based predictive modelling of micro gas turbine engine fuelled with microalgae blends on using LSTM networks: An experimental approach

Machine learning based predictive modelling of micro gas turbine engine fuelled with microalgae blends on using LSTM networks: An experimental approach

Yuchen Liu[a], V. Meenakshi[b], L. Karthikeyan[c], Josef Marousek[d,e,f], NR Krishnamoorthy[g], Manigandan Sekar[h,*], Omaima Nasif[i], Sulaiman Ali Alharbi[j], Yingji Wu[a], Changlei Xia[a,*]

[a]*Jiangsu Co-Innovation Center of Efficient Processing and Utilization of Forest Resources, International Innovation Center for Forest Chemicals and Materials, College of Materials Science and Engineering, Nanjing Forestry University, Nanjing, Jiangsu 210037, China*

[b]*Department of Electrical and Electronics Engineering, Sathyabama institute of science and technology, Chennai 600 119, India*

[c]*Department of Mechanical Engineering, Panimalar Engineering College, Chennai 600123, India*

[d]*Institute of Technology and Business in Ceské Budejovice, Faculty of Technology (Okružní 517/10, České Budějovice, 370 01, Czech Republic) e University of South Bohemia in České Budějovice, Faculty of Agriculture (Studentská 1668, České Budějovice, 370 05, Czech Republic)*

[f]*Tomas Bata Univesity in Zlín, Faculty of Management and Economics (Mostní 5139, Zlín, 760 01, Czech Republic)*

[g]*Department of Electronics and Instrumentation Engineering Sathyabama Institute of Science and Technology, Chennai 600 119, India*

[h]*Department of Aeronautical Engineering Sathyabama Institute of Science and Technology, Chennai 600 119, India*

[i]*Department of Physiology, College of Medicine and King Khalid University Hospital, King Saud University, Medical City, PO Box-2925, Riyadh 11461, Saudi Arabia*

[j]*Department of Botany and Microbiology, College of Science, King Saud University, PO Box -2455, Riyadh 11451, Saudi Arabia*

[*]*Corresponding authors: E-mail addresses: manisek87@gmail.com (M. Sekar), changlei.xia@njfu.edu.cn (C. Xia).*

ABSTRACT

Air transport plays an inevitable role in the transportation sector. In the modern world, the aviation contribution is very immense to establish worldwide developments. However, the emission released by the aviation industry is massively high. Due to the sudden increase in the air traffic the contribution of global CO_2 and CO have increased in recent years. Hence the aviation sector seeks the replacement for fossil fuels. In this study, the micro gas turbine engine has been experimentally studied for different engine speeds and throttle position. The gas turbine was allowed to run in the different test fuels such as, Jet-A, A20 (20% microalgae 80% Jet-A) and A30 (30% microalgae 70% Jet-A) and the predicted results were compared. In addition to the typical experimental calibrations, machine learning has been applied to examine the differences in the both performance and emission characteristics of the biofuel

blends with approximately 51 different fuel combinations using LSTM networks. Based on the predicted results, introduction of the biofuel affects the production of the static thrust. On the contrary, the emissions of the CO and CO_2 were very low compared to Jet-A. With regard to the nitrogen of the oxides, no massive reduction has been witnessed despite running at different fuel conditions. Besides, the marginal decrease in the NOx was observed above 75000 rpm.

Keywords: Microalgae, biofuel, jet engines, gas turbine engines, emission, machine learning

1. Introduction

The circumstance of the forthcoming year shows very clearly that most of the Conventional types of oil reserves used currently might get depleted completely by the next 30 years. This scenario globally causes the researchers to urge in replacing fossil fuel with more alternative energy, that could be renewable and available abundantly [**1-3**]. Consequently, the energy crisis in this modern world can be only be contended by developing alternate energy. Researchers believed such a huge energy demand can be fulfilled by bio-based energy resources. Initially, the first-generation biofuels were extracted from edible crops, but it was stopped completely due to scarcity in human intake. Thereby, the second-generation biofuels were extracted from the non-edible crops and they were much suitable and acceptable from the policymakers and researchers globally [**4-6**]. But economically, it seems to have a lot of disadvantages and constraints in the production of biofuel by utilizing non-edible crops. These crops have to be cultivated in fertile lands with proper irrigation techniques. Apart from that, they have certain dependencies on climate, soil type, human resources, machinery, etc as well as it seems to be a hugely time-consuming process. However, in commercial-scale biodiesel production environmental health-related issues like excess use of inorganic fertilizers, eutrophication is the major constraints [**7-10**]. Now if look at the economic side of biofuel production through non-edible crops seem too much costlier than the production cost of fossil fuel. Some of the important mentions of second-generation fuel with lignocellulosic biomass like cooking oil, agricultural waste, wood and forestry residues, solid waste from municipalities, etc provided better results [**11,12**]. But to obtain them economically for the mass and bulk production of biofuels, these resources failed to meet the demand. So, researchers globally need alternative third-generation biofuel feedstocks from the producing biofuel from non-edible oils, which could be economically good. Now researchers have identified microalgae as the third-generation biofuel, due to their feasibility and reliability in higher growth rate compared to that of the lignocellulosic based biofuel [**13,14**].

Algae oil could be the best substitute for these crops-based oils, due to their abundance as well as their ability to sustain in all types of water environment. Compared with terrestrial plants, microalgae have the great capacity of fixing the carbon dioxide by photosynthesis microorganism from the atmosphere to fetch biofuels efficiently through the extraction in the form of lipids [**15**]. Microalgal biomass production depends more on cultural techniques and nutrients, as well as lipid production, which can be optimised by stress induction. The microalgal seem to have good potential for lipid and carbohydrate contents. They have a very good ability to grow faster on wastewater, saline or seawater to give a good yield. For dairy wastewater remediation, poly-microalgae cultures that consist of green microalgae and cyanobacteria seem to be more promising than mono-microalgae cultures. Alage oil could be the best substitute for these crops-based oils, due to their abundance as well as their ability to sustain in saltwater [**16,17**]. The NOx emission of microalgal seems to be lowered with low compression ratios. The current study examines the effect of microalgae blends in the engine at different engine speed and throttle position. Although there were plenty of works related to the algae blends in the neat fossil fuel, the article related to the gas turbines were inadequate. In addition to

that, the prediction of the microgas turbines engine performance via machine learning techniques were limited to authors knowledge. Hence this study examines the opportunities of microalgae blends in the aviation sectors.

2. Materials and methods

2.1. Biodiesel preparation

The microalgae are one of the promising sources for production of the biofuel. Production of the biofuel from the microalgae expected to be sustainable options. Basically, the microalgae were produced by several methods. Oil pressing expected to the cheap and most reliable method. Here the microalgae were squeezed to produce the bio-oil. The produced biooil undergoes the process called transesterification where the byproduct glycerol was extracted from the bio-oil [**18,19**]. The automatic shaker had been used at continuous interval in separation of the unwanted products and filtered. Another popular method for the biofuel production is the use of hexane. Here, the obtained microalgae oil was mixed with hexane and cleaner for foreign objects and dust particles. During the usage the hexane is evaporated and the obtained fuel can be used as blend [**20,21**]. In the current study the simple oil pressing method has been used and the transesterification method was employed for the production of biofuel. **Table 1** shows the properties of the test fuel.

2.2. Experimental setup

The series of tested conducted in the micro level gas turbine engine which has ability to generate the trust of 178 N at the maximum with the rated speed of 87000 rpm.

Table 1 Engine specifications.

Engine type	Gas turbine
Size	Bench type
Rated thrust	178 N
Combustion	Single can
Compressor/Turbine	Impeller/ Axial
Fuel system	Piston
Rated speed	87000 rpm

Since it is an micro level setup, single stage radial compressor has been utilized. Here, the fuel inlet manifold has been modified to pass two types of fluid blends at required concentration. **Table 2** represents the specification of the engine. The major moving parts in the test setup is compressor and turbine. The flowmeter used to check to ensure fuel flow at the required rates [**22-24**]. To examine the temperature, k-type thermocouple sensor has been used. The samples are tested at different throttle position and engine speed. For each type of fuel, the test setup allows to run at least for 10 min in ideal to avoid the possibility of uncertainties in instrumentation and measurements. Further, the different reservoir was used to ensure the high reliability while testing. To measure the emission of the CO, HC and NOx, AVL Flame Ionization Detector has been used. All the gathered data were optimized and measured using the LABView linked with the data acquisition system (DAS).

2.3. Overview of LSTM networks

Long Short-Term Memory network is a type of Recurrent Neural Network (RNN) which has capability of learning long term dependencies. It is widely used in various applications such as signal processing, medical application and other forecasting application. The networks were invented by Hochreiter and Schmidhuber in the year 1997 [**25**]. Basically, all RNN networks consists of multiple layers with a single tanh function in a layer. In the LSTM network apart from tanh function, it also includes sigmoid function, multiplier and addition. These components are connected and result in four different functions namely input gate, output gate, cell candidate and forget gate. A simple LSTM architecture is shown in the **Fig. 1**. The first component in the LSTM is the cell state. It works like a conveyor belt flow from one state C_{t-1} to C_t which is shown at top of the **Fig. 1**. The next state C_t is depending on the linear interactions of forget state and cell state. The output of the multiplier is purely based on the gates output [**26**]. All gate consists of a sigmoid function and point-wise multiplication operation and works like a switch. Value of '1' in the sigmoid layer allows the data to pass through and '0' blocks the data from one stage to another. It has tendency to add or remove information to the network layer.

Forget gate layer is the second component in the LSTM layer. It looks for the h_{t-1} and xt value and fires the output as 0 or 1 to the variable f_t. The mathematical expression is given as.

$$f_t = \sigma(W_f.[h_{t-1}, x_t] + b_f) \quad (1)$$

W_f is the activation weight of the neurons and b_f is the bias value. The next component is update of cell state. A new cell stage $\hat{C}_t$is obtained from sigmoid function and update along with the input gate layer from sigmoid layer i_t.

Table 2 Properties of the biofuel.

Properties	Jet-A	B100 (100% microalgae oil)
Density kg/m3 @ 25 °C	802	852
Kinematic viscosity @ 40 °C	3.18	5.75
Calorific value (MJ/kg)	45.5	41.1
Flash point	37 °C	128 °C

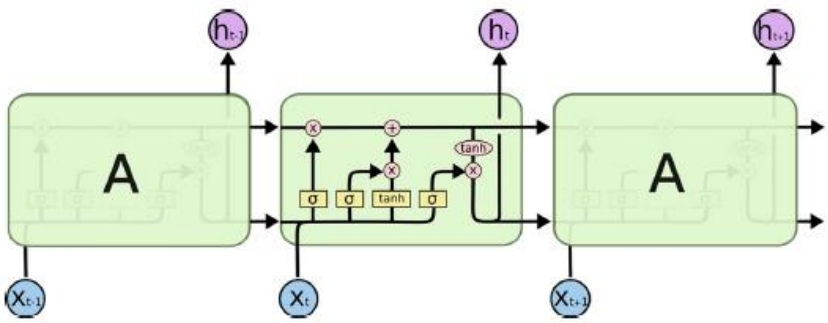

Fig. 1. LSTM network model.

These two value it and $\hat{C}_t$ are added and update of the state will be carried out. The mathematical expression for i_t and $\hat{C}_t$is shown below.

$$i_t = \sigma(W_i.[h_{t-1}, x_t] + b_i) \quad (2)$$

$$\widehat{C_t} = tanh(W_C.[h_{t-1}, x_t] + b_C) \quad (3)$$

The old cell state C_{t-1} is updated to the new cell state Ct by multiplying the forget state with the old state and adding the result with the new cell state $\hat{C}_t$ and it is mathematically expressed as.

$$C_t = f_t * C_{t-1} + i_t * \widehat{C_t} \quad (4)$$

In the final stage, the filter version of the updated cell state is fired as output. Sigmoid layer is applied to the current cell state Ct and it is multiplied with the output of tanh function to attain the final output cell state and it is represented as below.

$$O_t = \sigma(W_o[h_{t-1}, x_t] + b_o) \quad (5)$$

$$h_t = O_t * \tanh(C_t) \quad (6)$$

3. Results and discussion

3.1. Static thrust production

Fig. 2 represents the variation of the static thrust for various engine speed. Initially at the lower speed the production of static thrust is low, as the turbine speed increases the production of the thrust increased. At 30000 rpm, the fuel blends A20 and A30 reported 12 N and 11.5 N of thrust.

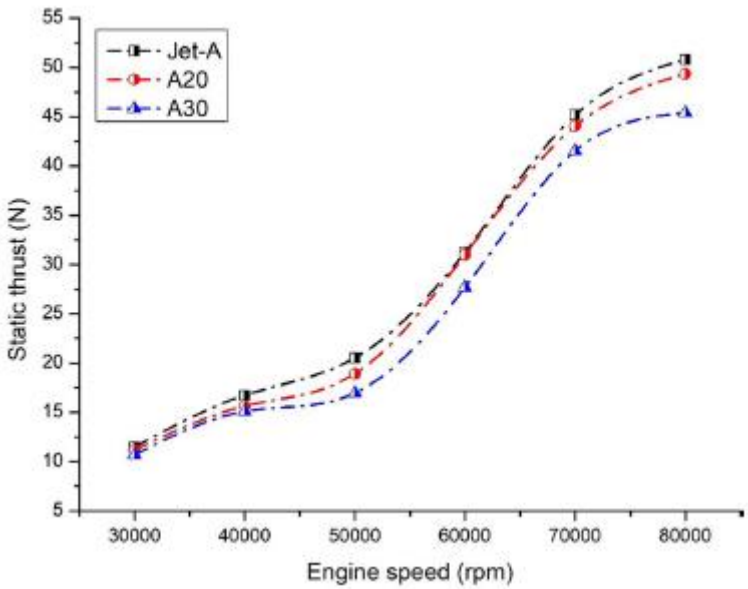

Fig. 2. Static thrust variation with respect to the gas turbine speed.

The difference between the all blends is not massive. Until the 40000 rpm, there is no significant difference between the samples Jet-A, A20 and A30 were observed. However, there is a profound increase in the thrust had been observed at 50000 rpm. Among the various blends, A20 reported 49.3 N of thrust at 80000 rpm. Compared to A30, A20 blend reported higher magnitude of static thrust

which is mainly due to the calorific value of the fuel. Typically, as the concentration of the blends to the Jet-A fuel increases, there is drastic reduction in the thrust has been noted [**7,27**]. **Fig. 3** shows the difference in the blends on production of thrust for different throttle position. From the observed results, it is clear there is no sign of improvements in the static thrust compared to the neat jet fuel. The dispersion of the Jet-A fuel with biofuel blends recorded poor thrust generation mainly due to the energy rate and heating value. On the other hand, the test blend A20 reported higher speeds for 20% and 40% throttle position compared to both A30 and Jet-A fuel. **Fig. 4** represents the change in the engine speed upon addition of the blends. From the figure it is very clear that, the increased concentration of the biofuel blends to the engine reduces the engine speed. The decisive reason for the above phenomenon is the reduction in the static thrust production by the engine when it is allowed to run on the alternate fuels.

3.2. Thrust specific fuel consumption

TSFC defined as the efficiency of the engine with respect to the amount of fuel consumed. As the engine speed increases the consumption of the fuel has been dropped massively. For instance, the consumption of the fuel at the 30000 rpm for the fuel samples Jet-A, A20 and A30 were 3.8 1/hr, 3.4 1/hr, and 3.39 1/hr which is 37%, 34% and 27.2% higher compared to 80000 rpm respectively.

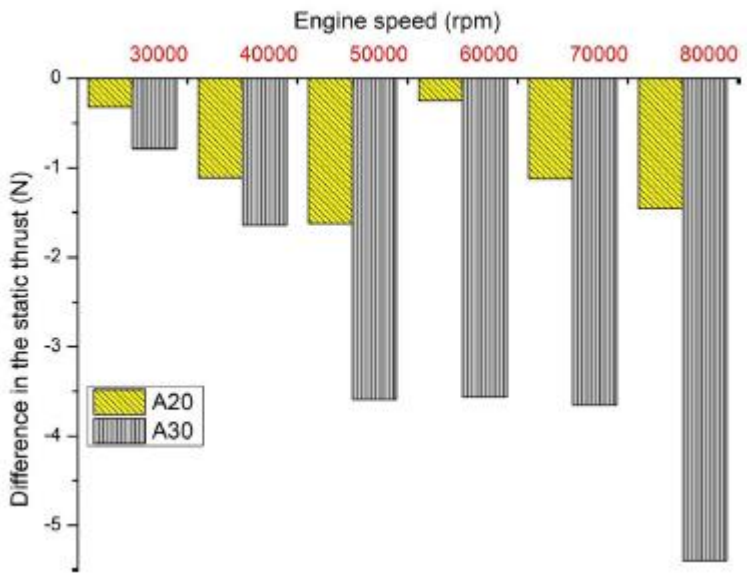

Fig. 3. Differences in the production of static thrust for biofuel compared to Jet-A fuel

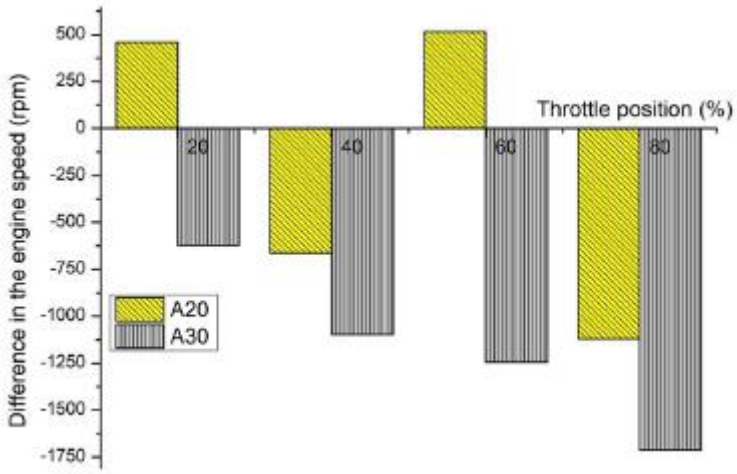

Fig. 4. Differences in the production of static thrust for biofuel compared to Jet-A fuel.

With regard to the lower consumption of the fuel, all blends reported the identical behaviour. The main reason for the reduced consumption at high speed was the complete combustion process. **Fig. 5** represents the three curves of the different sample at variety of engine speed. Even if the TSFC dropped relative to the engine speed, findings report the sharp decline in the TSFC from 30000 rpm to 55000 rpm and later the reduction in the consumption pattern is very sluggish and gradual. **Fig. 6** depicts the comparison of the fuel consumption patterns related to the Jet-A fuel. Irrespective of the engine speed all test blends reported higher consumption rate which is mainly due to the higher viscosity levels [**6,28**]. At higher engine speed, there is no big change in the consumption pattern has been observed between A20 and A30.

Emission characteristics

Emissions are the serious concerns for the environment. In the rapid world, burning of the fossil fuels were increased due to the increased demand in aviation vehicles. Approximately 15% of the global CO_2 were emitted by the aviation sectors. In this study the major emissions such as CO, CO_2 and NOx were inspected at different engine speeds. **Fig. 7** shows the variation of the CO with respect to the concentration of the biofuel blends. The maximum CO emission has been observed at 30000 rpm for all test blends. As the engine speed increased the emissions of the CO were dropped. The main reason for the reduction in the CO emissions were complete combustion and reduced fuel flow to the combustion chamber [**29,30**]. Compared to all blends A30 reported lower CO emission rate which is mainly due to the presence of higher oxygen molecules in the fuel. For instance, compared to the Jet-A, the blends A20 and A30 reported reduced emission levels. The emission levels of the Jet-A, A20 and A30 were 138 g/kg, 102.44 g/kg, and 93.5 g/kg at 30000 rpm and it is decreased as the engine speed increases to 80000 rpm. The comparative difference between the higher and lower speeds were 71%, 73% and 71.5% reduction in the total CO emission. Fig. 8 picturize the differences in the CO emission compared to the Jet-A fuel.

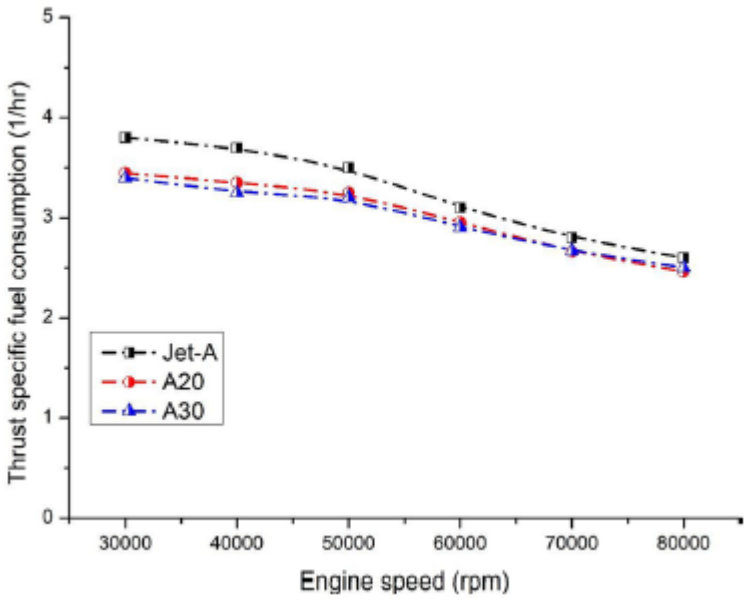

Fig. 5. Thrust specific fuel consumption with respect to the gas turbine speed.

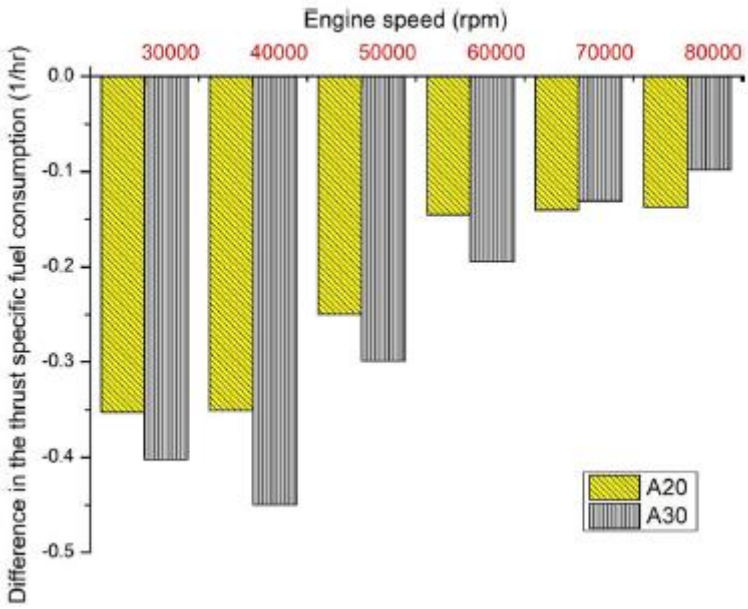

Fig. 6. Differences in the thrust specific fuel consumption for biofuel compared to Jet-A fuel.

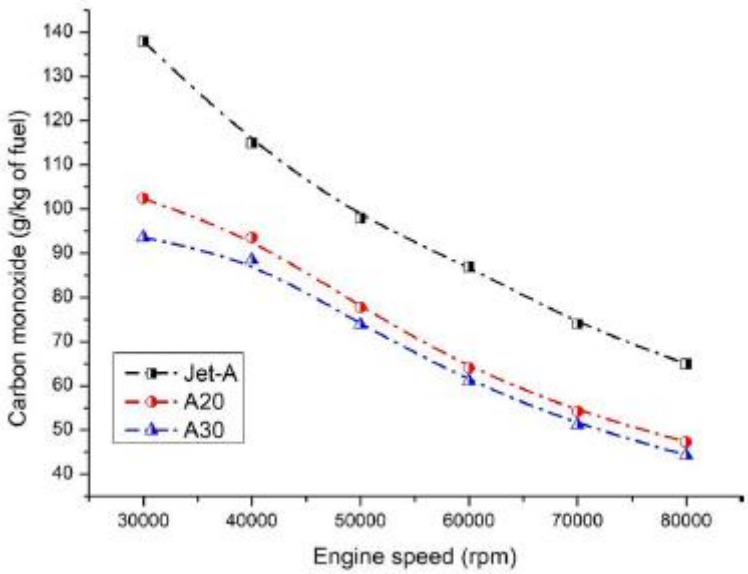

Fig. 7. Carbon monoxide emission with respect to the gas turbine speed.

Fig. 9 shows the change in the CO_2 with respect to the various engine speeds. As the engine speed increases there is gradual drop in the concentration of the CO_2. On the contrary, there is an slight increase in the CO_2 were noted at higher engine speed. Initially the values of the CO_2 were 3020 g/kg, 2955 g/kg and 2905 g/kg and decreased to 2980 g/kg, 2856 g/kg and 2807 g/kg at 60000 rpm. The maximum CO_2 production were witnessed at 80000 rpm and the minimum at 60000 rpm. The main reason for the increased emissions at the higher rpm is due to excess oxygen content present in the fuel [**22,31**]. To examine the difference in the engine speed and emission pattern **Fig. 10** shows only the changes compared to the Jet-A fuel. From the findings it is clear, regardless of the engine speed all the blends recorded reduced emissions. In particular, the blend A30 report higher reduction rates of CO_2.

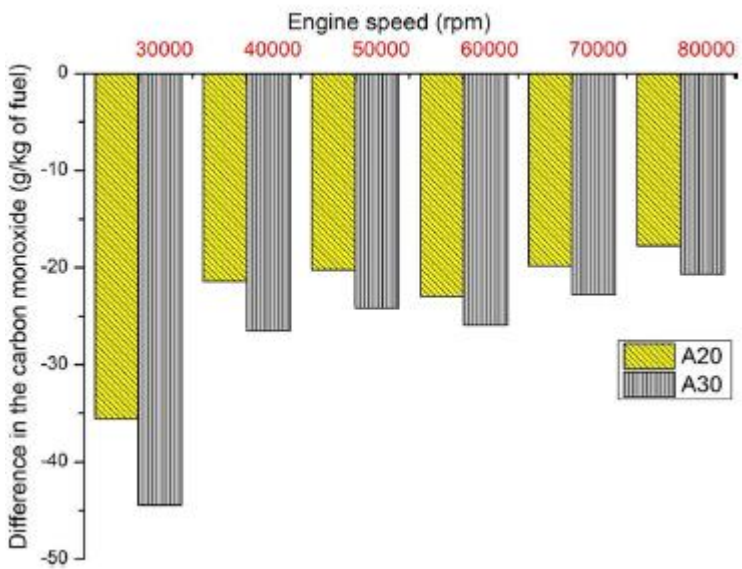

Fig. 8. Differences in emissions of carbon monoxide for biofuel compared to Jet-A fuel.

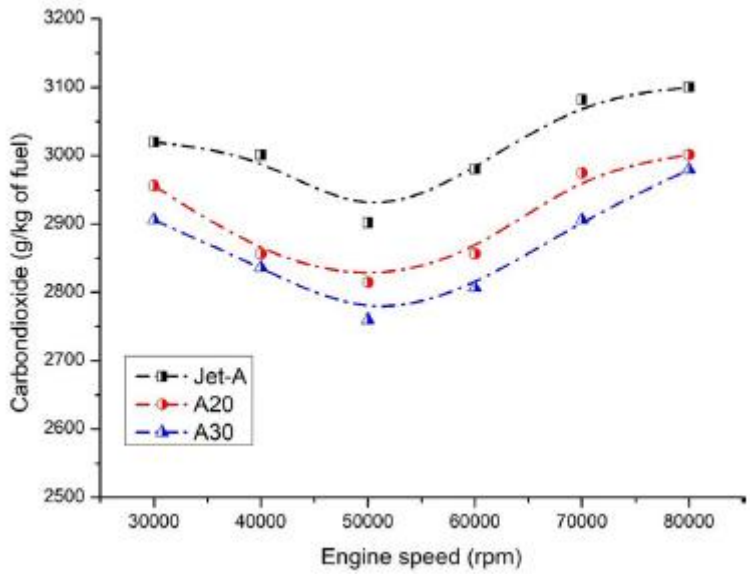

Fig. 9. Carbon dioxide emission variation with respect to the gas turbine speed.

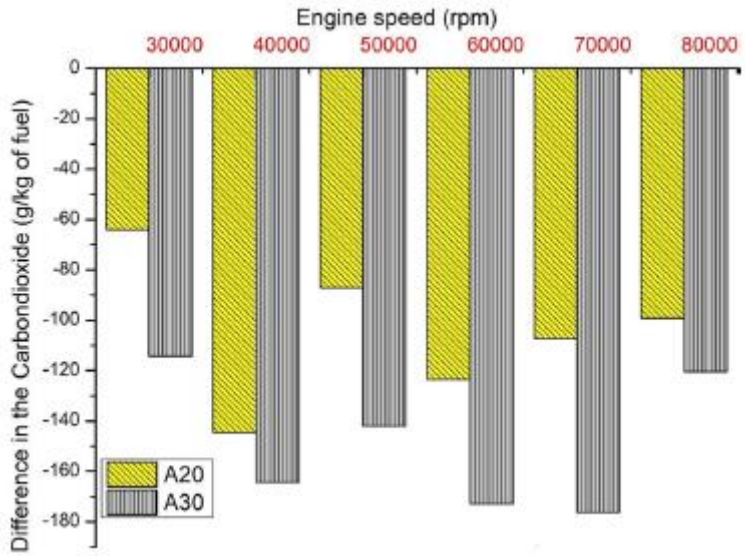

Fig. 10. Differences in emissions of carbon dioxide for biofuel compared to Jet-A fuel.

4. Machining learning approach on the test blends

Regression model along with LSTM network is proposed to generate the jet engine dataset. **Tables 3-10** shows RPM of jet engine at different throttle position. Using regression model, a sample data from **Table 1** is taken and polynomial expression is modelled initially. As an example, for throttle position of 20, jet engine type A result in the RPM of value of [35000, 35460, 34376.5] with chemical composition (CC) as [0, 20, 30]. Using these datasets, a second order equation is formulated as

$$\mathrm{RPM} = -4.378*(\mathrm{CC}*\ \mathrm{CC}) + 110.57*\ \mathrm{CC} + 35000\ (7).$$

Using the above equation, 300 RPM samples are generated with CC value ranges from 0 to 3 in step of 0.01. An LSTM network with 100 neurons is trained with these 300 samples. During training phase, epochs of 100 with 50 batch size are considered. The trained network is extrapolated to forecast the RPM value from 3 to 99 in step of 3 and it is listed in the **table 2**. The performance of LTSM network can be examined by comparing the RPM value of jet engine A at CC value of 20 and 30. It is observed that LSTM network forecast the RPM value as 35460.2 and 34376.9 against the actual value of 35,450 and 34376.5. The above phenomenon has been applied to fuel flow rate (**table 3**), static thrust (**table 4**), thrust specific fuel consumption (**table 5**), turbine temperature (**table 6**), carbon monoxide (**table 7**), carbon dioxide (**table 8**), and nitrogen of oxides (**table 9**). From the table 3-9 the different fuel combinations has been observed using the machine learning tool form LSTM network.**Table 10**..

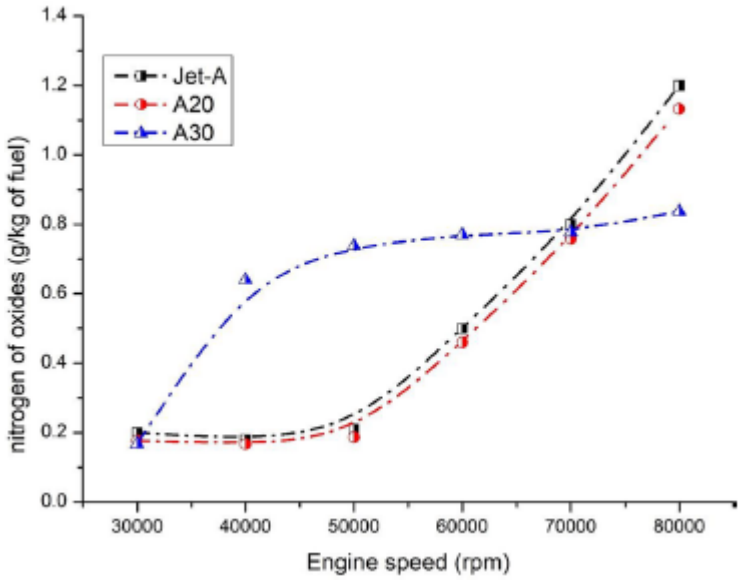

Fig. 11. Nitrogen of oxides emission with respect to the gas turbine speed.

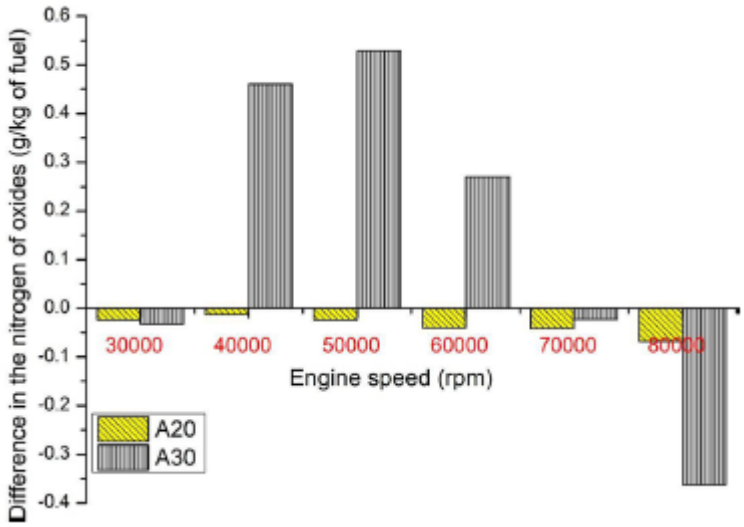

Fig. 12. Differences in emissions of carbon dioxide for biofuel compared to Jet-A fuel.

5. Conclusion

In this study the microalgae blends (A20 and A30) were tested for the static thrust, thrust specific fuel consumption, CO, CO_2 and NOx and procured results were compared with Jet-A fuel. From the series of tests conducted at different engine speeds, the throttle position and the engine speeds are related to each other. Typically, the maximum engine speed is achieved at the largest throttle position. The production of the static thrust increases as the engine speed is elevated. To be precise, the maximum static thrust production has been witnessed at higher engine speed of80000 rpm for samples Jet-A, A20 and A30 stood 50.8 N, 49.3 N and 45.4 N. As the concentration of the biofuel blend increases the static thrust dropped significantly. Hence, A30 reported least production of the static thrust at wide engine speeds. On the contrary, the amount of the fuel consumed by the engine is low for the A30 blends compared to Jet-A fuel. The foremost reason for the reduced TSFC was higher viscosity values. With regard to emissions both the CO and CO_2 pollutants for the blends A20 and A30 were very less than Jet-A fuel. When the biofuel blends dispersed with the regular Jet-A fuel the oxygen content in the fuel increases hence leads to the complete combustion. However, the NOx reported the contrary results compared to the other pollutants. Among the different blends A20 reported the lower emission rates. On the other hand, increased concentration of the biofuel blends stimulated the oxides of nitrogen, which is a typical behaviour. To analyse the performance and emission, the machine learning was performed with 51 different combinations and the adequate results. From the above argument it is very apparent that the use of the biofuel is sustainable in the aviation sectors with slight modification to the injection system in the micro gas turbine engine.

Table 3 Engine speed (rpm) data generated using LSTM network.

Fuel	20% Throttle		40% Throttle		60% Throttle		80% Throttle	
Type	A20	A30	A20	A30	A20	A30	A20	A30
3	0.2	0.2	0.4	0.3	0.6	0.6	0.8	0.8
6	0.2	0.2	0.4	0.3	0.6	0.5	0.8	0.7
9	0.2	0.2	0.3	0.3	0.6	0.5	0.8	0.7
12	0.2	0.2	0.3	0.3	0.5	0.5	0.8	0.7
15	0.2	0.2	0.3	0.3	0.5	0.5	0.7	0.6
18	0.2	0.2	0.3	0.3	0.5	0.5	0.7	0.6
20	0.2	0.1	0.3	0.3	0.5	0.5	0.7	0.6
21	0.2	0.1	0.3	0.3	0.5	0.5	0.7	0.6
24	0.2	0.1	0.3	0.3	0.5	0.5	0.6	0.6
27	0.2	0.1	0.3	0.3	0.5	0.4	0.6	0.6
30	0.1	0.1	0.3	0.3	0.4	0.4	0.6	0.6
33	0.1	0.1	0.3	0.3	0.4	0.4	0.5	0.6
36	0.1	0.1	0.3	0.3	0.4	0.3	0.5	0.6
39	0.1	0.1	0.3	0.2	0.3	0.3	0.4	0.6
42	0.1	0.1	0.3	0.2	0.3	0.3	0.4	0.6
45	0.1	0.1	0.3	0.2	0.3	0.2	0.3	0.6
48	0.0	0.1	0.2	0.2	0.2	0.2	0.2	0.6
51	0.0	0.1	0.2	0.2	0.2	0.1	0.2	0.6

Table 4 Fuel flow volume (L/min) data generated using LSTM network.

Fuel	20% Throttle		40% Throttle		60% Throttle		80% Throttle	
Type	A20	A30	A20	A30	A20	A30	A20	A30
3	11.5	11.7	16.6	16.8	20.5	20.4	31.8	31.0
6	11.5	11.8	16.4	16.8	20.4	20.3	32.1	30.7
9	11.5	11.8	16.2	16.7	20.2	20.0	32.2	30.4
12	11.4	11.6	16.1	16.4	19.9	19.6	32.1	30.1
15	11.3	11.4	15.9	16.0	19.6	19.2	31.9	29.7
18	11.3	11.1	15.7	15.6	19.2	18.7	31.4	29.4
20	11.2	10.8	15.6	15.2	18.9	18.3	31.0	29.1
21	11.1	10.7	15.6	15.0	18.8	18.1	30.8	29.0
24	11.0	10.2	15.4	14.3	18.2	17.4	29.9	28.6
27	10.9	9.6	15.3	13.5	17.6	16.6	28.9	28.1
30	10.7	8.8	15.1	12.6	16.9	15.7	27.7	27.7
33	10.5	8.0	15.0	11.6	16.2	14.8	26.3	27.2
36	10.4	7.1	14.8	10.5	15.4	13.7	24.7	26.7
39	10.1	6.1	14.6	9.3	14.5	12.6	22.9	26.2
42	9.9	4.9	14.5	8.0	13.5	11.4	20.9	25.6
45	9.7	3.7	14.3	6.5	12.5	10.1	18.8	25.1
48	9.4	2.4	14.2	5.0	11.4	8.8	16.4	24.5
51	9.1	1.0	14.0	3.3	10.2	7.3	13.9	23.9

Table 5 Static thrust (N) data generated using LSTM network.

Fuel	20% Throttle		40% Throttle		60% Throttle		80% Throttle	
Type	A20	A30	A20	A30	A20	A30	A20	A30
3	11.5	11.7	16.6	16.8	20.5	20.4	31.8	31.0
6	11.5	11.8	16.4	16.8	20.4	20.3	32.1	30.7
9	11.5	11.8	16.2	16.7	20.2	20.0	32.2	30.4
12	11.4	11.6	16.1	16.4	19.9	19.6	32.1	30.1
15	11.3	11.4	15.9	16.0	19.6	19.2	31.9	29.7
18	11.3	11.1	15.7	15.6	19.2	18.7	31.4	29.4
20	11.2	10.8	15.6	15.2	18.9	18.3	31.0	29.1
21	11.1	10.7	15.6	15.0	18.8	18.1	30.8	29.0
24	11.0	10.2	15.4	14.3	18.2	17.4	29.9	28.6
27	10.9	9.6	15.3	13.5	17.6	16.6	28.9	28.1
30	10.7	8.8	15.1	12.6	16.9	15.7	27.7	27.7
33	10.5	8.0	15.0	11.6	16.2	14.8	26.3	27.2
36	10.4	7.1	14.8	10.5	15.4	13.7	24.7	26.7
39	10.1	6.1	14.6	9.3	14.5	12.6	22.9	26.2
42	9.9	4.9	14.5	8.0	13.5	11.4	20.9	25.6
45	9.7	3.7	14.3	6.5	12.5	10.1	18.8	25.1
48	9.4	2.4	14.2	5.0	11.4	8.8	16.4	24.5
51	9.1	1.0	14.0	3.3	10.2	7.3	13.9	23.9

Table 6 Thrust specific fuel consumption (1/hr) speed data generated using LSTM network.

Fuel	20% Throttle		40% Throttle		60% Throttle		80% Throttle	
Type	A20	A30	A20	A30	A20	A30	A20	A30
3	3.7	3.7	3.6	3.6	3.4	3.4	3.1	3.0
6	3.7	3.6	3.6	3.4	3.4	3.3	3.0	3.0
9	3.6	3.4	3.5	3.3	3.4	3.3	3.0	2.9
12	3.5	3.4	3.5	3.2	3.3	3.2	3.0	2.9
15	3.5	3.3	3.4	3.1	3.3	3.2	3.0	2.8
18	3.5	3.2	3.4	3.1	3.3	3.1	3.0	2.8
20	3.4	3.2	3.3	3.1	3.3	3.1	3.0	2.8
21	3.4	3.2	3.3	3.0	3.2	3.1	2.9	2.7
24	3.4	3.2	3.3	3.0	3.2	3.1	2.9	2.7
27	3.4	3.1	3.3	3.0	3.2	3.1	2.9	2.7
30	3.4	3.1	3.2	3.0	3.2	3.1	2.9	2.7
33	3.4	3.2	3.2	3.1	3.2	3.1	2.9	2.6
36	3.4	3.2	3.2	3.1	3.2	3.1	2.9	2.6
39	3.4	3.2	3.2	3.2	3.2	3.1	2.9	2.6
42	3.4	3.3	3.2	3.3	3.2	3.1	2.9	2.6
45	3.5	3.4	3.2	3.4	3.2	3.1	2.9	2.6
48	3.5	3.5	3.2	3.5	3.2	3.2	2.9	2.6
51	3.6	3.6	3.2	3.7	3.3	3.2	2.9	2.6

Table 7 Turbine temperature (K) data generated using LSTM network.

Fuel	20% Throttle		40% Throttle		60% Throttle		80% Throttle	
Type	A20	A30	A20	A30	A20	A30	A20	A30
3	740.3	724.4	727.1	716.5	753.1	744.8	797.9	787.7
6	739.1	710.6	726.2	707.1	748.9	733.9	789.1	770.5
9	736.4	698.5	724.2	698.7	744.4	724.4	780.4	755.5
12	732.3	688.1	721.2	691.3	739.7	716.3	772.0	742.7
15	726.7	679.4	717.2	685.0	734.8	709.5	763.8	732.0
18	719.7	672.5	712.2	679.7	729.6	704.1	755.8	723.5
20	714.1	668.8	708.2	676.7	725.9	701.3	750.6	719.0
21	711.1	667.2	706.1	675.4	724.1	700.1	748.0	717.2
24	701.1	663.7	699.0	672.2	718.4	697.5	740.4	713.0
27	689.6	661.9	690.8	670.0	712.5	696.3	733.1	711.0
30	676.7	661.9	681.7	668.8	706.3	696.4	725.9	711.2
33	662.3	663.5	671.5	668.7	699.8	697.9	719.0	713.5
36	646.4	666.9	660.2	669.6	693.1	700.8	712.3	718.0
39	629.0	672.0	647.9	671.6	686.1	705.0	705.8	724.6
42	610.2	678.8	634.6	674.6	678.9	710.7	699.6	733.4
45	589.9	687.3	620.3	678.6	671.5	717.7	693.5	744.4
48	568.2	697.6	604.9	683.7	663.8	726.1	687.7	757.6
51	544.9	709.6	588.6	689.8	655.8	735.8	682.0	772.9

Table 8 Carbon monoxide (g/kg) speed data generated using LSTM network.

Fuel	20% Throttle		40% Throttle		60% Throttle		80% Throttle	
Type	A20	A30	A20	A30	A20	A30	A20	A30
3	3013.5	2991.2	2970.4	2957.5	2890.9	2871.2	2959.4	2939.3
6	3005.9	2965.0	2942.9	2918.1	2879.1	2843.4	2939.5	2903.0
9	2997.2	2941.3	2918.6	2882.7	2866.6	2818.5	2920.3	2870.9
12	2987.4	2920.2	2897.5	2851.4	2853.5	2796.7	2901.9	2843.2
15	2976.6	2901.6	2879.5	2824.1	2839.6	2777.8	2884.3	2819.8
18	2964.6	2885.5	2864.7	2800.8	2825.1	2762.0	2867.4	2800.8
20	2956.0	2876.2	2856.5	2787.5	2815.0	2753.1	2856.5	2790.5
21	2951.5	2872.0	2853.0	2781.6	2809.9	2749.1	2851.2	2786.1
24	2937.4	2861.0	2844.4	2766.4	2793.9	2739.2	2835.8	2775.7
27	2922.1	2852.6	2839.1	2755.2	2777.3	2732.3	2821.2	2769.6
30	2905.8	2846.7	2836.8	2748.1	2760.0	2728.4	2807.3	2767.8
33	2888.4	2843.3	2837.8	2745.1	2742.0	2727.5	2794.1	2770.4
36	2869.9	2842.5	2841.8	2746.0	2723.4	2729.6	2781.7	2777.3
39	2850.2	2844.2	2849.1	2751.0	2704.0	2734.7	2770.1	2788.5
42	2829.5	2848.5	2859.5	2760.1	2683.9	2742.7	2759.2	2804.1
45	2807.7	2855.3	2873.0	2773.2	2663.2	2753.8	2749.1	2823.9
48	2784.8	2864.7	2889.7	2790.3	2641.8	2767.8	2739.7	2848.1
51	2760.9	2876.6	2909.6	2811.5	2619.6	2784.8	2731.0	2876.7

Table 9 Carbon dioxide (g/kg) speed data generated using LSTM network

Fuel Type	20% Throttle		40% Throttle		60% Throttle		80% Throttle	
	A20	A30	A20	A30	A20	A30	A20	A30
3	131.2	127.1	110.8	108.8	93.9	92.2	82.1	81.4
6	124.8	117.5	107.0	103.2	90.2	86.9	77.7	76.3
9	119.1	109.2	103.5	98.2	86.9	82.1	73.8	71.9
12	113.8	102.2	100.3	93.8	83.9	77.8	70.5	68.1
15	109.1	96.4	97.5	90.1	81.3	74.1	67.6	65.0
18	104.9	91.9	95.0	87.0	79.1	70.8	65.3	62.4
20	102.4	89.6	93.6	85.2	77.8	68.9	64.0	61.1
21	101.3	88.7	92.9	84.5	77.2	68.1	63.5	60.5
24	98.2	86.7	91.1	82.6	75.7	65.9	62.1	59.2
27	95.6	86.0	89.6	81.3	74.6	64.2	61.3	58.6
30	93.6	86.6	88.5	80.7	73.9	63.0	61.0	58.5
33	92.1	88.5	87.7	80.7	73.5	62.4	61.2	59.1
36	91.1	91.6	87.3	81.3	73.5	62.2	62.0	60.3
39	90.7	96.0	87.2	82.6	73.8	62.6	63.2	62.1
42	90.8	101.7	87.4	84.5	74.5	63.5	65.0	64.5
45	91.4	108.7	88.0	86.9	75.6	64.9	67.2	67.5
48	92.6	116.9	88.9	90.1	77.1	66.8	70.0	71.2
51	94.3	126.4	90.1	93.8	78.9	69.3	73.3	75.5

Table 10 Nitrogen of oxides (g/kg) speed data generated using LSTM network

Fuel Type	20% Throttle		40% Throttle		60% Throttle		80% Throttle	
	A20	A30	A20	A30	A20	A30	A20	A30
3	0.2	0.2	0.1	0.3	0.1	0.3	0.4	0.6
6	0.2	0.2	0.0	0.4	0.0	0.4	0.4	0.6
9	0.2	0.2	0.0	0.5	0.0	0.5	0.4	0.7
12	0.2	0.2	0.0	0.5	0.0	0.6	0.4	0.8
15	0.2	0.2	0.1	0.6	0.1	0.7	0.4	0.8
18	0.2	0.2	0.1	0.6	0.1	0.8	0.4	0.8
20	0.2	0.2	0.2	0.6	0.2	0.8	0.5	0.9
21	0.2	0.2	0.2	0.6	0.2	0.8	0.5	0.9
24	0.2	0.2	0.3	0.6	0.4	0.9	0.6	0.9
27	0.2	0.2	0.5	0.6	0.5	0.9	0.7	0.9
30	0.2	0.2	0.6	0.6	0.7	0.9	0.8	1.0
33	0.2	0.2	0.8	0.5	1.0	0.9	0.9	1.0
36	0.2	0.1	1.1	0.5	1.2	0.9	1.1	1.0
39	0.2	0.1	1.3	0.4	1.6	0.9	1.2	1.0
42	0.2	0.1	1.6	0.3	1.9	0.9	1.4	1.0
45	0.2	0.1	1.9	0.2	2.3	0.9	1.6	1.0
48	0.2	0.2	0.1	0.3	0.1	0.3	0.4	0.6
51	0.2	0.2	0.0	0.4	0.0	0.4	0.4	0.6

References

[1] Torres S, Acien G, García-Cuadra F, Navia R. Direct transesterification of microalgae biomass and biodiesel refining with vacuum distillation. Algal Res 2017;28:30-8.

[2] Jandačka J, Mižieta J, Holubčík M, Nosek R. Experimental determination of bed temperatures during wood pellet combustion. Energy Fuels 2017;31(3):2919-26.

[3] Maroušek J, Trakal L. Techno-economic analysis reveals the untapped potential of wood biochar. Chemosphere 2022;291:133000.

[4] Pasupuleti RR, Tsai PC, Ponnusamy VK. Low-cost disposable Poly(ethyleneimine)-functionalized carbon nanofibers coated cellulose paper as efficient solid phase extraction

sorbent material for the extraction of parahydroxybenzoates from environmental waters. Chemosphere 2021;267:129274.

[5] Sekar M, Ponnusamy VK, Pugazhendhi A, Nižetic S, Praveenkumar TR. Production and utilization of pyrolysis oil from solidplastic wastes: A review on pyrolysis process and influence of reactors design. J Environ Manage 2022;302:114046.

[6] Devi B, S. V, Vimal R, T.r. P. Influence of high oxygenated biofuels on micro-gas turbine engine for reduced emission. Aircr Eng Aerosp Tec 2021;93(3):508-13.

[7] Anderson A, Karthikeyan A, Ramachandran S, Praveenkumar TR. Lowest emission sustainable aviation biofuels as the potential replacement for the Jet-A fuels. Aircr Eng Aerosp Tec 2021;93(3):502-7.

[8] Ge S, Manigandan S, Mathimani T, Basha S, Xia C, Brindhadevi K, et al. An assessment of agricultural waste cellulosic biofuel for improved combustion and emission characteristics. Sci Total Environ 2022;813:152418.

[9] Al-Kheraif AA, Syed A, Elgorban AM, Divakar DD, Shanmuganathan R, Brindhadevi K. Experimental assessment of performance, combustion and emission characteristics of diesel engine fuelled by combined non-edible blends with nanoparticles. Fuel 2021;295:120590.

[10] Van Hung T, Alkhamis HH, Alrefaei AF, Sohret Y, Brindhadevi K. Prediction of emission characteristics of a diesel engine using experimental and artificial neural networks. Appl Nanosci 2021:1. https://doi.org/10.1007/s13204-021-01781-z.

[11] Orejuela-Escobar LM, Landázuri AC, Goodell B. Second generation biorefining in Ecuador: Circular bioeconomy, zero waste technology, environment and sustainable development: The nexus. J Bioresour Bioprod 2021;6(2):83-107.

[12] Patel A, Shah AR. Integrated lignocellulosic biorefinery: Gateway for production of second generation ethanol and value added products. J Bioresour Bioprod 2021;6 (2):108-28.

[13] Xia C, Brindhadevi K, Elfasakhany A, Alsehli M, Tola S. Performance, combustion and emission analysis of castor oil biodiesel blends enriched with nanoadditives and hydrogen fuel using CI engine. Fuel 2021;306:121541.

[14] Xia C, Brindhadevi K, Elfasakhany A, Alsehli M, Tola S. Numerical modelling of the premixed compression ignition engine for superior combustion and emission characteristics. Fuel 2021;306:121540.

[15] Ge S, Brindhadevi K, Xia C, Khalifa AS, Elfasakhany A, Unpaprom Y, et al. Enhancement of the combustion, performance and emission characteristics of spirulina microalgae biodiesel blends using nanoparticles. Fuel 2022;308:121822.

[16] Muthuraman RM, Murugappan A, Soundharajan B. Highly effective removal of presence of toxic metal concentrations in the wastewater using microalgae and pretreatment processing. Appl Nanosci 2021. https://doi.org/10.1007/s13204-021-01795-7.

[17] Piloni RV, Daga IC, Urcelay C, Moyano EL. Experimental investigation on fast pyrolysis of freshwater algae. Prospects for alternative bio-fuel production. Algal Res 2021;54:102206.

[18] Zorn SMFE, Reis CER, Bento HBS, de Carvalho AKF, Silva MB, De Castro HF. In situ transesterification of marine microalgae biomass via heterogeneous acid catalysis. BioEnergy Res 2020;13(4):1260-8.

[19] Singh N, Kumar K, Goyal A, Moholkar VS. Ultrasound-assisted biodiesel synthesis by in-situ transesterification of microalgal biomass: Optimization and kinetic analysis. Algal Res 2022;61:102582.

[20] Namitha B, Sathish A, Kumar PS, Nithya K, Sundar S. Micro algal biodiesel synthesized from Monoraphidium sp., and Chlorella sorokiniana: Feasibility and emission parameter studies. Fuel 2021;301:121063.

[21] Zou X, Xu K, Chang W, Qu Y, Li Y. Rapid extraction of lipid from wet microalgae biomass by a novel buoyant beads and ultrasound assisted solvent extraction method. Algal Res 2021;58:102431.

[22] Manigandan S, Atabani AE, Ponnusamy VK, Gunasekar P. Impact of additives in Jet-A fuel blends on combustion, emission and exergetic analysis using a micro-gas turbine engine. Fuel 2020;276:118104.

[23] Nithya S. Impact of nanofluids on combustion and emission characteristic of the micro gas turbine. Int J Ambient Energy 2020. https://doi.org/10.1080/ 01430750.2020.1818122.

[24] Boomadevi P, Paulson V, Samlal S, Varatharajan M, Sekar M, Alsehli M, et al. Impact of microalgae biofuel on microgas turbine aviation engine: A combustion and emission study. Fuel 2021;302:121155.

[25] Hochreiter S, Schmidhuber J. Flat minima. Neural Comput 1997;9:1-42.

[26] Barman PP, Boruah A. A RNN based approach for next word prediction in assamese phonetic transcription. Procedia Comput Sci 2018;143:117-23.

[27] Habib Z, Parthasarathy R, Gollahalli S. Performance and emission characteristics of biofuel in a small-scale gas turbine engine. Appl Energy 2010;87(5):1701-9.

[28] Seljak T, Katrasnik T. Emission reduction through highly oxygenated viscous biofuels: use of glycerol in a micro gas turbine. Energy 2019;169:1000-11.

[29] Allouis C, Amoresano A, Capasso R, Langella G, Niola V, Quaremba G. The impact of biofuel properties on emissions and performances of a micro gas turbine using combustion vibrations detection. Fuel Process Technol 2018;179:10-6.

[30] Mendez CJ, Parthasarathy RN, Gollahalli SR. Performance and emission characteristics of butanol/Jet A blends in a gas turbine engine. Appl Energy 2014; 118:135-40.

[31] Devi PB, Joseph DR, Gokulnath R, Manigandan S, Gunasekar P, Anand TP, et al. The effect of TiO2 on engine emissions for gas turbine engine fueled with jatropha, butanol, soya and rapeseed oil. Int J Turbo Jet Eng 2020;37(1):85-94.

[32] Thanh NC, Askary AE, Elfasakhany A, Nithya S. Exergy and energy analyses of the Spirulina microalgae blends in a direct injection engine at variable engine loads. J Energy Res Technol 2021;143(12):120908.

[35] Su M, Li W, Ma Q, Zhu B. Production of jet fuel intermediates from biomass

platform compounds via aldol condensation reaction over iron-modified MCM-41 lewis acid zeolite. J Bioresour Bioprod 2020;5(4):256-65.